Journal of Molecular Structure 990 (2011) 183–196

Contents lists available at ScienceDirect

Journal of Molecular Structure

journal homepage: www.elsevier.com/locate/molstruc

Interactions of amino acids, carboxylic acids, and mineral acids with different quinoline derivatives

Dipjyoti Kalita, Himangshu Deka, Shyam Sundar Samanta, Subrata Guchait, Jubaraj B. Baruah *

Department of Chemistry, Indian Institute of Technology Guwahati, Guwahati, 781 039 Assam, India

ARTICLE INFO

Article history:
Received 8 December 2010
Received in revised form 19 January 2011
Accepted 19 January 2011
Available online 26 January 2011

Keywords:
Amides
Quinoline
Acid recognition
Amino acids
Fluorescence
Crystal structures

ABSTRACT

A series of quinoline containing receptors having amide and ester bonds are synthesized and characterised. The relative binding abilities of these receptors with various amino acids, carboxylic acids and mineral acids are determined by monitoring the changes in fluorescence intensity. Among the receptors bis(2-(quinolin-8-yloxy)ethyl) isophthalate shows fluorescence enhancement on addition of amino acids whereas the other receptors shows fluorescence quenching on addition of amino acids. The receptor N-(quinolin-8-yl)-2-(quinolin-8-yloxy) propanamide has higher binding affinity for amino acids. However, the receptor N-(quinolin-8-yl)-2-(quinolin-8-yloxy)acetamide having similar structure do not bind to amino acids. This is attributed to the concave structure of the former which is favoured due to the presence of methyl substituent. The receptor bis(2-(quinolin-8-yloxy)ethyl) isophthalate do not bind to hydroxy carboxylic acids, but is a good receptor for dicarboxylic acids. The crystal structure of bromide and perchlorate salts of receptor 2-bromo-N-(quinolin-8-yl)-propanamide are determined. In both the cases the amide groups are not in the plane of quinoline ring. The structure of N-(quinolin-8-yl)-2-(quinolin-8-yloxy)acetamide, N-(2-methoxyphenethyl)-2-(quinolin-8-yloxy)acetamide and their salts with maleic acid as well as fumaric acid are determined. It is observed that the solid state structures are governed by the double bond geometry of these two acid. Maleic acid forms salt in both the cases, whereas fumaric acid forms either salt or co-crystals.

1. Introduction

Quinoline derivatives are used as drugs for different diseases such as tuberculosis, schizophrenia and malaria [1–7]. Apart from its medicinal value quinoline derivatives are also studied as a supramolecular host [8–13]. Several quinoline based receptors containing urea and amide functionality are known for their binding abilities with various anions. These receptors are selective towards smaller halide anions in comparison to the larger halide anions [8]. Various weak interactions such as π–π interaction, H-bond interaction govern the main architecture of these hosts [9,10]. As the quinoline group is a Lewis base, the nitrogen atom of the ring can be easily protonated to form its salt and such hosts can be used as cationic receptors for anions. The structural aspects, properties of salts and inclusion compounds of quinoline derivatives are also studied in details [11]. Quinoline derivatives such as 8-aminoquinoline and 8-hydroxyquinoline have also been used as guests with suitable hosts [12,13]. Our interest on study of quinoline based receptor is because of their medicinal value, ready availability of binding site, and the presence of a fluorophore group that makes solution study handy. Further to this there are different possibilities to functionalize such derivatives so that they have number of sites for weak interactions and also able to confer directional properties while self-assembly formation. We have been interested in the structural studies and molecular recognition of various anions by quinoline based receptors [14,15]. Many organic and inorganic receptors for recognition of amino acids are synthesized and their binding properties are studied. Most of these receptors have structures relatively difficult to synthesize or used in the form of metal complexes [16–21]. In this study we have focused our interest to understand the binding properties of different organic and inorganic acids towards quinoline derived receptors. For this purpose we have chosen a series of fluorescence active quinoline functionalised receptors listed in Chart 1.

Here we present a comparative binding abilities of different acids, namely amino acid, mineral acid and carboxylic acid with these quinoline based receptors by determining their binding constants and also showed that how such bindings takes place in solid state structures in their co-crystals and salts.

2. Experimental

All reagents and solvents were purchased commercially and were used without further purification, unless otherwise stated. ^{1}H NMR data were recorded with a Varian 400 MHz FT-NMR

* Corresponding author. Tel.: +91 361 2582311; fax: +91 361 2690762.
E-mail address: juba@iitg.ernet.in (J.B. Baruah).

0022-2860/$ - see front matter © 2011 Elsevier B.V. All rights reserved.
doi:10.1016/j.molstruc.2011.01.040

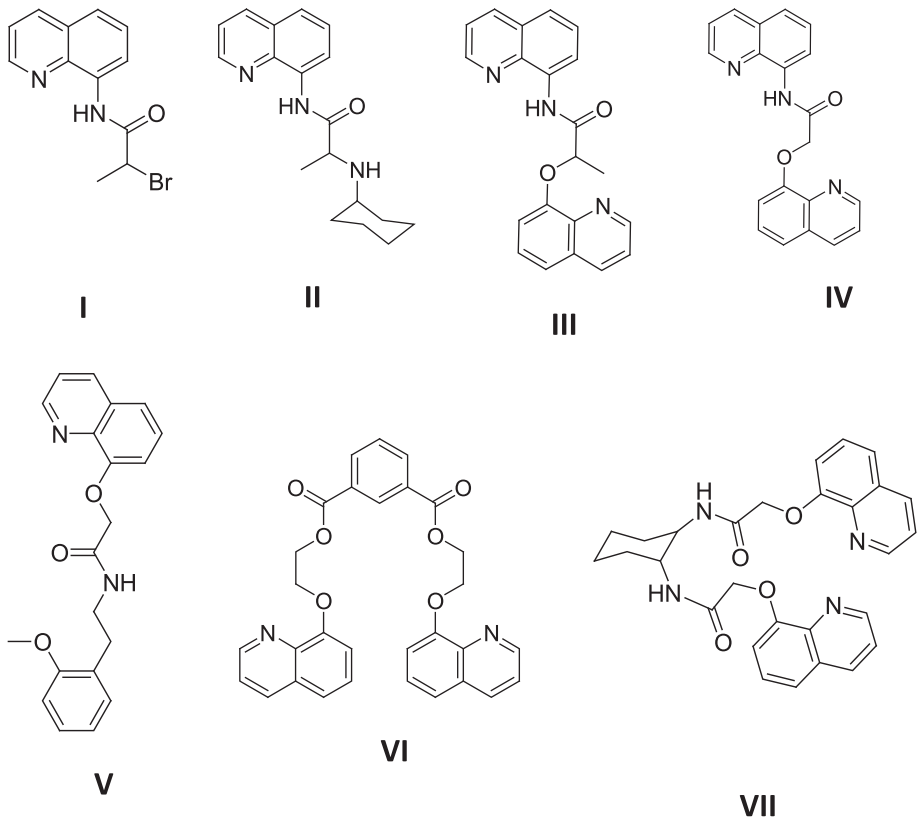

Chart 1. Various receptors used for acid binding studies.

spectrometer. The FT-IR spectra were recorded using a PerkinElmer spectrum one spectrometer in the KBr pellets in the range 4000–400 cm^{-1}. The UV/Vis spectra were recorded using a PerkinElmer Lambda 750 spectrometer. The fluorescence spectra were recorded with a PerkinElmer LS 55 fluorescence spectrophotometer. For the fluorescence titration, solutions of the compounds in methanol were prepared at definite concentrations (as described in each figure captions) and a constant aliquots (10 μL) of different guest acids (10^{-2} M in methanol) were added to the host solution. Fluorescence spectra of the solution were recorded after every addition of the guest acids. The binding constants were determined from the fluorescence titration curve as reported earlier for 1:1 host–guest complex formation [22].

2.1. Synthesis of 2-bromo-N-(quinolin-8-yl)propanamide (*I*)

To a solution of 8-aminoquinoline (0.433 g, 3 mmol) in dry dichloromethane (20 mL) triethylamine (0.31 g, 3 mmol) was added. The solution was stirred at 0 °C for 15 min and 2-bromopropionylbromide (0.316 g, 3 mmol) was added over a period of 30 min. The reaction mixture was then stirred overnight at room temperature. To the reaction mixture 20 ml of water was added and the organic layer was separated using a separatory funnel. The solution was then dried over anhydrous sodium sulphate and the solvent was removed under reduced pressure to obtain a brown solid. The crude product was then recrystallised from dichloromethane. Yield: 78%. IR (KBr, cm^{-1}): 3375 (b), 3042 (s), 3005 (s), 2949 (m), 2896 (m), 1689 (s), 1611 (w), 1587 (m), 1547 (s), 1494 (m), 1428 (s), 1389 (s), 1363 (s), 1245 (w), 1160 (w), 1038 (m), 834 (m), 777 (m). ^{1}H NMR ($CDCl_3$, 400 MHz): 12.01 (s, 1H); 9.78 (d, J = 5.6 Hz, 1H); 9.19 (d, J = 8.4 Hz, 1H); 8.21 (t, J = 8.4 Hz, 1H); 7.97 (d, J = 8.4 Hz, 1H); 7.89 (t, J = 7.6 Hz, 1H); 7.72 (d, J = 7.2 Hz, 1H); 6.12 (q, J = 6.4 Hz, 1H); 2.01 (d, J = 6.4 Hz, 3H).

2.2. Synthesis of the salt *Ia* and *Ib*

Compound **I** was dissolved in dilute solution of hydrobromic acid and perchloric acid and allowed to stand for 3 days to obtain the crystals of their respective salts (**Ia** and **Ib**). **Ia**: Yield 67%, IR (KBr, cm^{-1}): 3393 (bs), 2924 (m), 2851 (m), 1639 (m), 1558 (w), 1456 (m), 1378 (m), 1319 (m), 1157 (bm), 1052 (m), 1034 (m), 816 (m). **Ib**: Yield 67%, IR (KBr, cm^{-1}): 3433 (bs), 3265 (s), 1686 (s), 1644 (m), 1607 (m), 1566 (m), 1475 (m), 1371 (m), 1143 (s), 1120 (s), 1085 (s), 838 (m), 765 (m), 625 (m).

2.3. Synthesis of 2-(cyclohexylamino)-N-(quinolin-8-yl)propanamide (*II*)

2-bromo-N-(quinolin-8-yl)propanamide (**I**) (0.834 g, 3 mmol), cyclohexylamine (0.297 g, 3 mmol) and potassium carbonate (0.5 g, 3.7 mmol) were taken in dry tetrahydrofuran (20 mL) and stirred at 70 °C for 9 h (progress of the reaction was monitored at regular intervals using TLC). After completion of the reaction, the product was filtered and the solvent was removed under reduced pressure. The product **II** was further purified by thin layer chromatography (silica gel; hexane/ethyl acetate 3:2). Yield: 48%. IR (KBr, cm^{-1}): 3329 (b), 2927 (m), 2851 (m), 1672 (s), 1520 (s), 1486 (m), 1448 (w), 1423 (w), 1382 (w), 1322 (m), 1130 (m), 1052 (m), 823 (m), 791 (m). ^{1}H NMR ($CDCl_3$, 400 MHz): 11.62 (s, 1H); 8.86 (d, J = 6.0 Hz, 1H); 8.82 (d, J = 7.2 Hz, 1H); 8.15 (d, J = 8.0 Hz, 1H); 7.51 (m, 2H); 7.42 (m, 1H); 3.51 (q, J = 6.8 Hz, 1H); 2.50 (d, J = 3.6 Hz, 1H); 2.03 (bs, 1H); 1.63 (m, 4H); 1.46 (d, J = 6.8 Hz, 3H); 1.13 (m, 6H). ^{13}C NMR ($CDCl_3$): 20.9, 25.2, 25.3, 26.2, 33.9,

33.3, 56.5, 57.1, 116.5, 121.7, 127.5, 128.3, 134.8, 136.3, 136.6, 139.4, 148.6, 175.3. LC–MS [M + 1]: 298.20.

2.4. Synthesis of N-(quinolin-8-yl)-2-(quinolin-8-yloxy) propanamide (*III*)

The 2-bromo-N-(quinolin-8-yl)propanamide (1.36 g, 5 mmol) was dissolved in dry acetone (30 ml). To the reaction mixture K_2CO_3 (1.0 g, 7.5 mmol) was added and stirred for 20 min. Then 8-hydroxyquinoline (0.725 g, 5 mmol) was added and the reaction mixture was refluxed at 70 °C for 10 h. (Progress of the reaction was monitored at regular intervals using TLC.) After completion of the reaction, the reaction mixture was filtered to remove the K_2CO_3. The solvent from the filtrate was then removed under reduced pressure to obtain the crude product which was further purified by thin layer chromatography (silica gel; hexane/ethyl acetate 3:2). Yield: 48%. IR (KBr, cm^{-1}): 3432 (m), 3257 (s), 2764 (s), 1704 (s), 1637 (w), 1516 (s), 1420 (m), 1384 (m), 1309 (m), 1281 (m), 1218 (s), 1163 (m), 1063 (w), 993 (w), 873 (w), 821 (s),777 (w), 609 (m). ^{1}H NMR ($CDCl_3$, 400 MHz): 11.2 (s, 1H), 9.0 (d, J = 4.0 Hz, 1H), 8.8 (d, J = 7.2 Hz, 1H), 8.6 (d, J = 4.4 Hz, 1H), 8.1 (d, J = 8.4 Hz 1H), 8.0 (d, J = 8.4 Hz, 1H), 7.5–7.4 (m, 5H) 7.3 (m,1H), 7.2 (d, J = 7.2 Hz, 1H), 5.2 (q, J = 6.8 Hz, 1H), 1.9 (d, J = 6.8 Hz, 3H).

2.5. Synthesis of N-(quinolin-8-yl)-2-(quinolin-8-yloxy)acetamide *IV*

The compound was synthesized by a reported procedure [23].

2.6. Synthesis of the salt and co-crystals of maleic acid and fumaric acid (*Va*, *Vb*, *IVa*, and *IVb*)

The receptors were dissolved in aqueous methanol and the respective acids were added in 1:1 ratio. The solutions were then kept undisturbed for 3–4 days to obtain either the salts or the co-crystals.

IVa: Yield: 71%. IR (KBr, cm^{-1}): 3409 (bs), 1686 (s), 1545 (s), 1491 (w), 1427 (m), 1318 (s), 1274 (s), 1218 (m), 1011 (m), 825 (m), 645 (s).
IVb: Yield: 74%. IR (KBr, cm^{-1}): 3393 (bs), 1684 (m), 1603 (m), 1543 (s), 1490 (s), 1427 (w), 1364 (m), 1353 (m), 1315 (m), 1274 (w), 1191 (w), 1120 (w), 961 (w), 873 (m), 824 (m), 793 (m), 745 (w), 611 (m).

2.7. Synthesis of N-(2-methoxyphenethyl)-2-(quinolin-8-yloxy)acetamide (*V*)

2-(2-Methoxyphenyl)ethylamine (0.755 g, 5 mmol) was dissolved in dry dichloromethane (20 mL) and triethylamine (0.505 g, 5 mmol) was added to it. The solution was stirred at 0 °C for 15 min and bromoacetylbromide (0. 1.01 g, 5 mmol) was added to the stirred solution over a period of 30 min. The reaction mixture was stirred overnight at room temperature. It was then filtered to remove the hydrobromide salts, and the filtrate was removed under reduced pressure. The corresponding amide obtained was recrystallised from dichloromethane. In the next step, the amide obtained (1.08 g, 5 mmol), 8-hydroxyquinoline (0.725 g, 5 mmol) and potassium carbonate (1.0 g, 7.5 mmol) were taken in dry acetone (20 mL) and the reaction mixture was stirred at 60 °C for 9 h (progress of the reaction was monitored at regular intervals using TLC). After completion of the reaction, the reaction mixture was filtered and the solvent was removed under reduced pressure. The product obtained was purified by column chromatography. Yield: 54%. IR (KBr, cm^{-1}): 3360 (bs), 3051 (s), 2968 (w), 1642 (s), 1601 (m), 1552 (s), 1504 (s), 1497 (s), 1469 (s), 1433 (m), 1380 (m), 1315 (s), 1264 (m), 1251 (s), 1115 (s), 1034 (m), 826 (m), 757 (s). ^{1}H NMR ($CDCl_3$, 400 MHz): 8.8 (d, J = 4 Hz,

Table 1
Crystallographic parameter for compounds.

Compound no.	Ia	Ib	IV	IVa	IVb	V	Va	Vb
Formulae	$C_{12}H_{12}Br_2N_2O$	$C_{12}H_{12}BrClN_2O_5$	$C_{20}H_{15}N_3O_2$	$C_{26}H_{23}N_3O_9$	$C_{24}H_{20}N_3O_7$	$C_{20}H_{24}N_2O_5$	$C_{24}H_{24}N_2O_7$	$C_{22}H_{21}N_2O_5$
CCDC no.	781136	781137	790481	790482	790480	790478	790479	790477
Mol. wt.	360.06	379.60	329.35	521.47	462.43	372.41	452.45	393.41
Crystal system	Triclinic	Monoclinic	Triclinic	Triclinic	Monoclinic	Triclinic	Monoclinic	Monoclinic
Space group	P-1	P2(1)/n	P-1	P-1	P2(1)/n	P-1	P2(1)/n	P2(1)/c
Temperature/K	296	296	296	296	296	296	296	296
Wavelength/Å	0.71073	0.71073	0.71073	0.71073	0.71073	0.71073	0.71073	0.71073
a/Å	7.5545(5)	5.0946(2)	8.2758(7)	7.5146(7)	6.7151(11)	8.7292(14)	17.862(3)	17.792(15)
b/Å	9.8698(8)	28.4639(9)	10.0169(8)	12.2378(12)	16.530(3)	10.675(2)	4.8456(8)	4.909(4)
c/Å	10.1227(8)	10.0728(3)	10.2197(9)	13.6349(13)	19.258(4)	11.0402(19)	26.550(4)	25.985(16)
α/°	62.797(4)	90.00	85.635(5)	94.239(7)	90.00	87.703(10)	90.00	90.00
β/°	79.255(4)	101.073(2)	85.319(5)	97.921(7)	91.372 (6)	72.230(8)	101.540(9)	120.21 (4)
γ/°	80.067(4)	90.00	77.445(5)	97.873(6)	90.00	80.940(9)	90.00	90.00
V/Å^3	656.21(9)	1433.49(8)	822.69(12)	1224.7(2)	2136.9(6)	967.4(3)	2251.6(6)	1961 (3)
Z	2	4	2	2	4	2	4	4
Density/Mg m^{-3}	1.822	1.759	1.330	1.414	1.437	1.278	1.335	1.332
Abs. Coeff./mm^{-1}	6.162	3.076	0.088	0.109	0.108	0.092	0.099	0.095
F(0 0 0)	352	760	344	544	964	396	952	828
Total no. of reflections	3224	3459	2927	4365	3850	3282	3866	3423
Reflections, $I > 2\sigma(I)$	2446	1815	2336	2087	1763	2747	1418	1967
Max. 2θ/°	56.84	56.70	50.5	50.5	50.5	50.0	50.5	50.5
Ranges (h, k, l)	$-10 \le h \le 10$ $-13 \le k \le 13$ $-13 \le l \le 13$	$-6 \le h \le 6$ $-37 \le k \le 30$ $-11 \le l \le 13$	$-9 \le h \le 9$ $-11 \le k \le 11$ $-12 \le l \le 12$	$-8 \le h \le 8$ $-14 \le k \le 13$ $-16 \le l \le 16$	$-7 \le h \le 8$ $-19 \le k \le 19$ $-22 \le l \le 23$	$-10 \le h \le 10$ $-12 \le k \le 12$ $-9 \le l \le 13$	$-21 \le h \le 21$ $-5 \le k \le 4$ $-29 \le l \le 27$	$-21 \le h \le 20$ $-5 \le k \le 5$ $-30 \le l \le 31$
Complete to 2θ (%)	97.8	96.7	98.4	98.5	99.6	96.8	94.8	96.5
Refinement method	Full-matrix least-squares on F^2	Full-matrix least-squares on F^2	Full-matrix least-squares on F^2	Full-matrix least-squares on F^2	Full-matrix least-squares on F^2	Full-matrix least-squares on F^2	Full-matrix least-squares on F^2	Full-matrix least-squares on F^2
Data/Restraints/Parameters	2446/0/159	1815/0/195	2927/0/226	4365/0/357	3850/4/319	3282/0/265	3866/0/311	3423/0/273
Goof (F^2)	1.075	0.951	1.041	0.871	1.059	0.855	0.765	0.679
R indices [$I > 2\sigma(I)$]	0.0572	0.0508	0.0574	0.0409	0.0998	0.0589	0.0493	0.0529
R indices (all data)	0.0717	0.1024	0.0653	0.0958	0.1612	0.0654	0.1454	0.2053

1H); 8.2 (d, J = 8.4 Hz, 1H); 7.4 (m, 2H); 7.0 (d, J = 7.2 Hz, 2H), 6.9 (d, J = 7.2 Hz, 1H); 6.7 (m, 2H); 4.7 (s, 2H); 3.7 (s, 3H); 3.5 (t, J = 6.8 Hz, 2H); 2.8 (t, J = 7.2 Hz, 2H); 2.2 (bs, 1H). ^{13}C NMR ($CDCl_3$): 30.3, 39.4, 55.3, 69.8, 110.4, 111.7, 120.5, 121.6, 122.1, 127.0, 127.5, 127.8, 129.7, 130.6, 136.5, 140.2, 149.4, 153.9, 157.7, 168.6. LC–MS [M + 1]: 337.17.

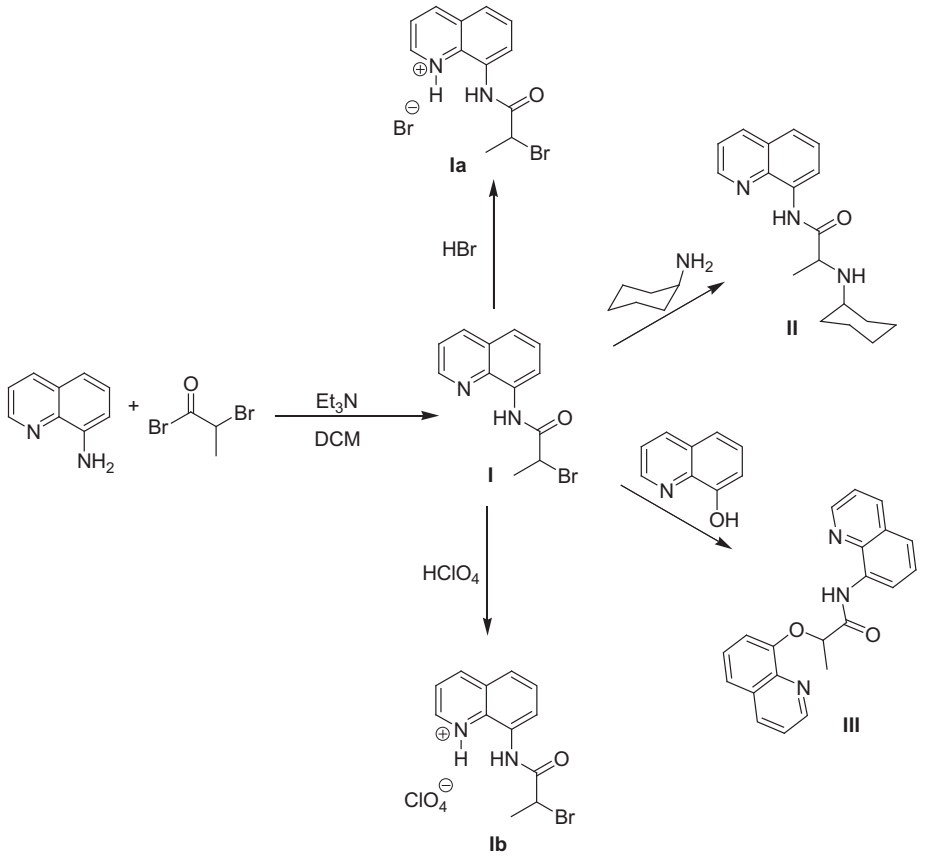

Scheme 1. Synthesis of 2-bromo-N-(quinolin-8-yl)propanamide (**I**) and its derivatives.

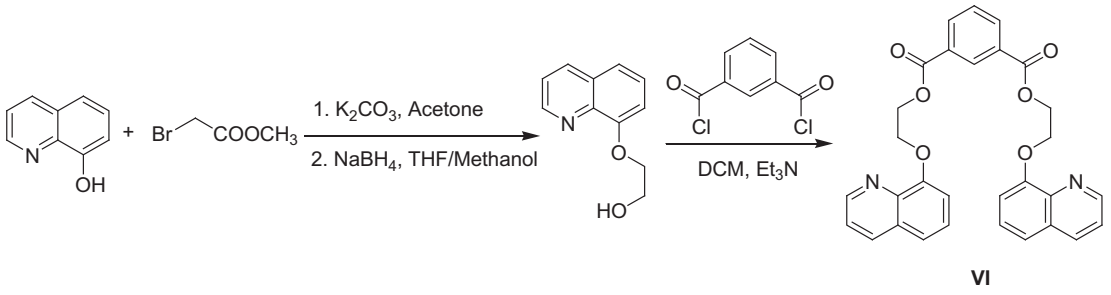

Scheme 2. Synthesis of compound **VI**.

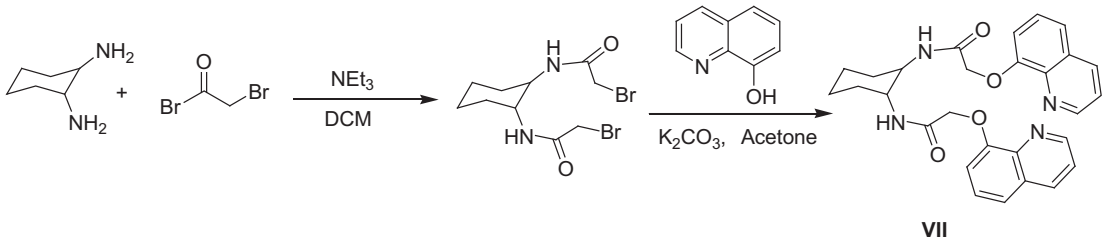

Scheme 3. Synthesis of compound **VII**.

Va: Yield: 74%. IR (KBr, cm^{-1}): 3433 (bs), 33,052 (s), 3056 (w), 3006 (w), 2940 (w), 1673 (s), 1618 (m), 1601 (m), 1495 (s), 1464 (s), 1348 (m), 1305 (m), 1280 (m), 1244 (m), 1111 (m), 1034 (w), 874 (w), 858 (m), 830 (m).
Vb: Yield: 77%. IR (KBr, cm^{-1}): 3388 (s), 2941 (w), 1703 (w), 1698 (w), 1672 (s), 1551 (m), 1508 (m), 1494 (m), 1424 (m), 1379 (m), 1296 (s), 1262 (s), 1245 (s), 1165 (m), 1111 (s), 1042 (m), 824 (m), 785 (m), 749 (s).

2.8. Synthesis of 2-(quinolin-8-yloxy) ethanol

8-Hydroxyquinoline (.725 g, 5 mmol) was dissolved in dry acetone (20 ml) and potassium carbonate (1.0 g, 7.5 mmol) was added to it. The solution was stirred at room temperature for 15 min and then methyl bromoacetate (0.76 g, 5 mmol) was added and the reaction mixture was then refluxed at 70 °C for 12 h (Progress of the reaction was monitored at regular intervals using TLC). After completion of the reaction, the reaction mixture was then filtered and the solvent was then removed under reduced pressure to obtain the ester as a yellow solid. In the next step, the ester was reduced to the corresponding alcohol using a reported procedure [24]. Yield: 77%. IR (KBr, cm^{-1}): 3405 (b), 3175 (b), 2923 (m), 2861 (m), 1613 (w), 1505 (m), 1475 (m), 1381 (m), 1322 (m), 1266 (m), 1116 (m), 1075 (s), 904 (w), 823 (m). ^{1}H NMR ($CDCl_3$, 400 MHz): 8.8 (d, J = 4.4 Hz, 2 H), 8.0 (d, J = 8.4, 2H), 7.3 (m, 3H), 7.0 (d, J = 7.6 Hz, 1H), 4.2 (t, J = 4.8 Hz, 2H), 4.1 (t, J = 4.8 Hz, 2H), 3.4 (bs, 1H).

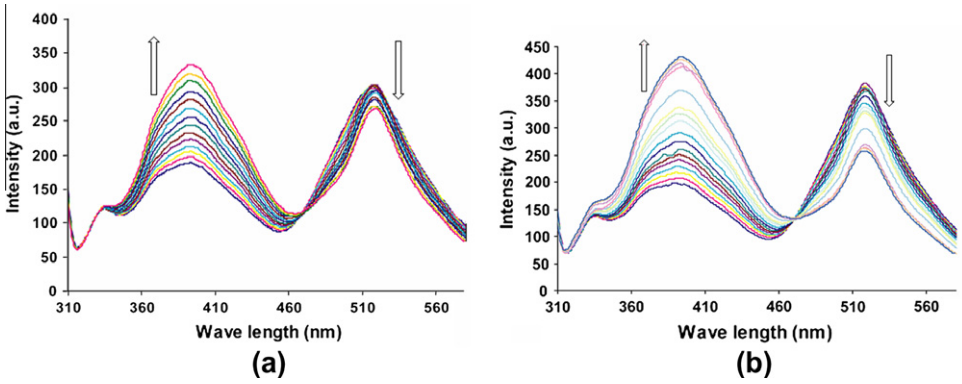

Fig. 1. Changes in emission spectra (λ_{ex} = 310 nm) of **I** (6.7×10^{-5} M in methanol); on addition of: (a) DL-alanine, (b) L-alanine (10^{-2} M in methanol in 10 μL aliquot).

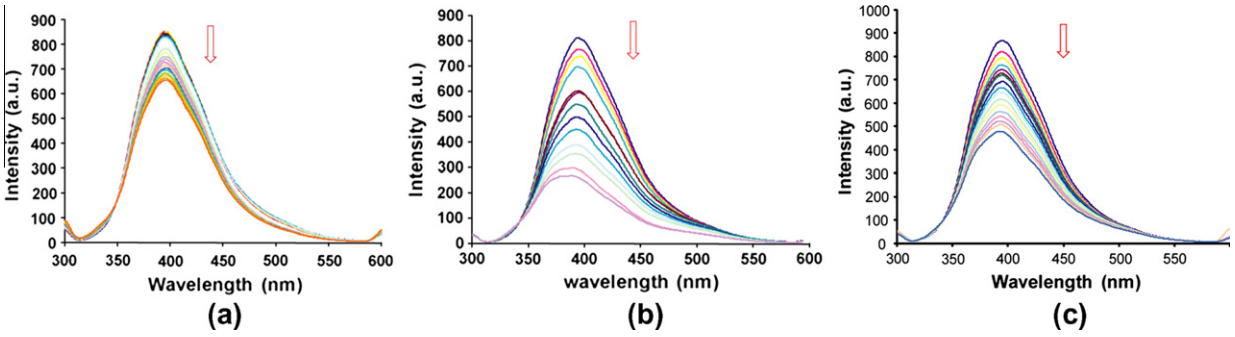

Fig. 2. Changes in fluorescence spectra (λ_{ex} = 310 nm) of **II** (1.26×10^{-4} M in methanol) on addition of: (a) glycine, (b) hydrochloric acid, (c) acetic acid (all 10^{-2} M in methanol, in 10 μL aliquot).

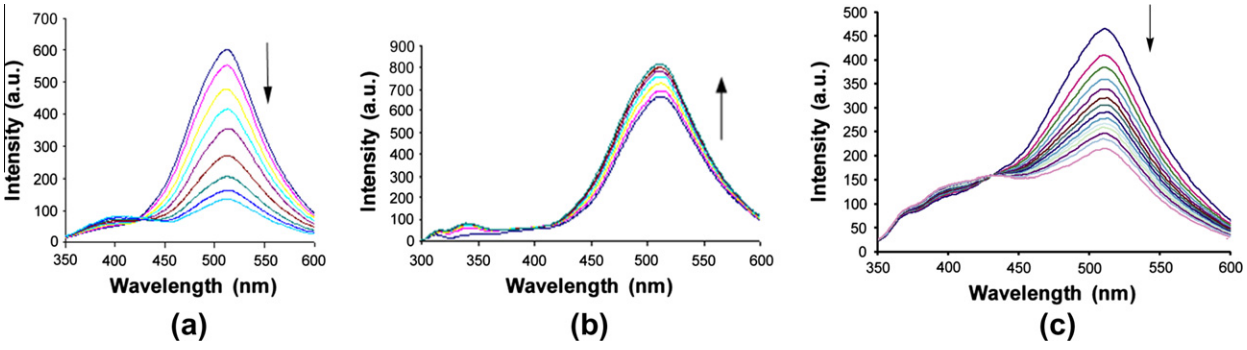

Fig. 3. Changes in fluorescence spectra of **III** (2.5×10^{-5} M in methanol) on addition of (a) glycine (10^{-2} M in methanol), (b) hydrochloric acid (10^{-2} M in methanol), (c) acetic acid (10^{-2} M in methanol, in 10 μL aliquot).

2.9. Synthesis of bis (2-(quinolin-8-yloxy)ethyl) isophthalate (**VI**)

The 2-(quinolin-8-yloxy)ethanol (0.756 g, 4 mmol) was dissolved in dry dichloromethane (20 ml) and triethylamine (0.404 g, 4 mmol) was added to it. The solution was stirred at 0 °C for 15 min and isophthaloyl dichloride (0.404 g, 2 mmol) was added to the stirred solution. The reaction mixture was then refluxed at 40 °C for 8 h (progress of the reaction was monitored at regular intervals using TLC). After completion of the reaction, 30 mL of water was added to the reaction mixture and the organic layer was separated using a separatory funnel. The solvent was then removed under reduced pressure to obtain a light yellow colour solid. The product was further purified by thin layer chromatography (silica gel; hexane/ethyl acetate 5:3). Yield: 73%. IR (KBr, cm^{-1}): 3422 (b), 2921 (w), 1720 (s), 1608 (w), 1508 (m), 1474 (w), 1451 (w), 1382 (m), 1259 (w), 1119 (m), 822 (w), 790 (w). ^{1}H NMR (DMSO-d^6, 400 MHz): 8.8(d, J = 2.8 Hz, 1H), 8.4 (s, 1H), 8.3(d, J = 8 Hz, 2H), 8.1(t, J = 6.4 Hz, 3H), 7.6 (t, J = 7.6 Hz, 2H), 7.5 (m, 5H), 7.3(t, J = 5.2 Hz, 2H), 4.7 (s, 4H), 4.5 (s, 4H). LC–MS (M + 1): 509.22.

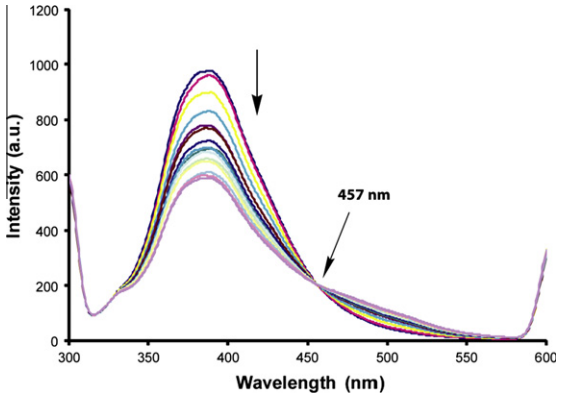

Fig. 4. Changes in fluorescence spectra of **V** (6.67×10^{-6} M in methanol) with maleic acid (10^{-2} M in methanol, in 10 μL aliquot).

2.10. Synthesis of ***VII***

Trans-1,2-diaminocylohexane (0.342 g, 3 mmol) was dissolved in dry dichloromethane (20 mL) and triethylamine (0.61 g, 6 mmol) was added to it. The solution was stirred at 0 °C for 15 min and bromoacetylbromide (1.212 g, 6 mmol) was added to the stirred solution over a period of 30 min. The reaction mixture was then stirred overnight at room temperature. To the reaction mixture 20 mL of water was added and the organic layer was separated using a separatory funnel. The solution was then dried over sodium sulphate and the solvent was removed under reduced pressure to obtain a brown solid. The crude product was then recrystallised from dichloromethane. The amide thus obtained (1.06 g, 3 mmol), 8-hydroxyquinoline (0.870 g, 6 mmol) and potassium carbonate (1.0 g, 7.4 mmol) were taken in dry tetrahydrofuran (20 mL) and the reaction mixture was stirred at 70 °C for 9 h (progress of the reaction was monitored at regular intervals using

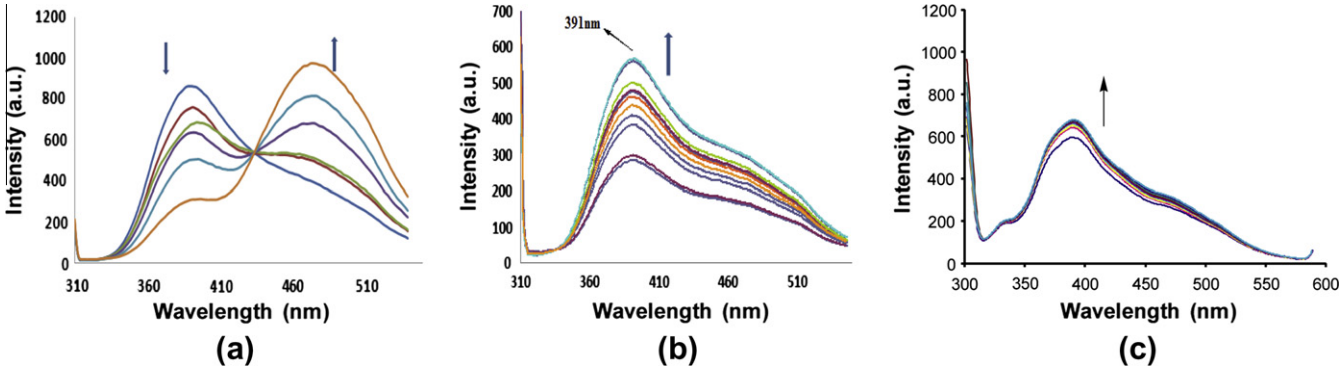

Fig. 5. Changes in fluorescence spectra (λ_{ex} = 310 nm) of **VI** (6.7×10^{-5} M in methanol) on addition of: (a) hydrochloric acid (10^{-2} M in methanol), (b) glycine (10^{-2} M in methanol). (c) Acetic acid (10^{-2} M in methanol, in 10 μL aliquot).

Table 2
Binding constant of different receptors calculated from fluorescence titration.

Guest	Binding constant (/mole)					
	II	**III**	**IV**	**V**	**VI**	**VII**
Glycine	8.058×10^3	3.825×10^6	[a]	[a]	6.478×10^5	[a]
Methionine	1.639×10^3	5.224×10^6	[a]	[a]	2.847×10^5	[a]
Hydrobromic acid	5.844×10^5	6.074×10^5	4.952×10^5	2.271×10^6	6.022×10^6	3.625×10^6
Hydrochloric acid	3.967×10^5	7.932×10^5	3.369×10^5	2.103×10^6	1.400×10^7	4.813×10^7
Perchloric acid	1.394×10^6	1.582×10^5	1.087×10^6	4.052×10^6	5.160×10^6	4.475×10^7
Acetic acid	1.22×10^5	1.388×10^6	1.055×10^5	[a]	$5.68\ 0 \times 10^4$	[a]
Fumaric acid	5.228×10^5	4.487×10^4	7.520×10^4	1.920×10^5	1.148×10^5	9.060×10^5
Maleic acid	9.811×10^5	1.464×10^4	1.329×10^6	4.963×10^6	2.822×10^6	2.399×10^7
L-Ascorbic acid	1.316×10^5	1.854×10^4	[a]	[a]	[a]	2.650×10^5
L-Mandelic acid	3.99×10^5	2.591×10^4	2.950×10^4	[a]	[a]	4.079×10^6
D-Mandelic acid	3.596×10^5	1.484×10^5	2.920×10^4	[a]	[a]	6.247×10^6
L-Tartaric acid	3.978×10^5	1.068×10^5	7.920×10^4	2.220×10^5	1.142×10^5	1.466×10^6

[a] No changes in fluorescence spectra on addition of guest.

TLC). After completion of the reaction, the product was filtered and the solvent was removed under reduced pressure. The product was further purified by thin layer chromatography. Yield: 57%. IR (KBr, cm^{-1}): 3465 (b), 2927 (m), 2856 (w), 1660 (s), 1551 (m), 1504 (m), 1474 (w), 1437 (w), 1378 (m), 1318 (m), 1260 (m), 1184 (w), 1112 (m), 785 (m), 751 (m). ^1H NMR ($CDCl_3$, 400 MHz): 8.92 (d, J = 4.4 Hz, 2H); 8.17 (d, J = 8.4 Hz, 2H); 7.50 (m, 2H); 7.42 (t, J = 8.4 Hz, 2H); 7.34 (t, J = 8.0 Hz, 2H); 6.98(d, J = 7.6 Hz, 2H); 4.64 (d, J = 14.8 Hz, 2H); 4.42 (d, J = 15.2 Hz, 2H); 3.95 (bs, 2H); 2.05 (m, 3H); 1.76 (m, 3H); 1.25 (m, 4H). ^{13}C NMR ($CDCl_3$): 25.0, 32.7, 52.5, 69.1, 102.2, 111.1, 121.4, 122.2, 126.9, 129.8, 136.7, 149.4, 168.6. LC–MS [M + 1]: 485.24.

2.11. Crystal structure determination

The X-ray single crystal diffraction data were collected at 296 K with Mo Kα radiation (λ = 0.71073 Å) using a Bruker Nonius SMART CCD diffractometer equipped with a graphite monochromator. The SMART software was used for data collection and also for indexing the reflections and determining the unit cell parameters; the collected data were integrated using SAINT software. The structures were solved by direct methods and refined by full-matrix least-squares calculations using SHELXTL software. All the non-H atoms were refined in the anisotropic approximation against F^2 of all reflections. The H-atoms, except those attached to oxygen atoms were placed at their calculated positions and refined in the isotropic approximation; those attached to oxygen were located in the difference Fourier maps, and refined with isotropic displacement coefficients. The crystallographic parameters of the compounds are tabulated in Table 1.

3. Results and discussion

3.1. Synthesis and characterisation of receptors

The compound 2-bromo-N-(quinolin-8-yl)propanamide (**I**) was synthesized by reacting 2-bromopropionylbromide with 8-aminoquinoline in dichlorometane in the presence of triethylamine (Scheme 1). The compound **I** was transformed to various derivatives such as 2-(cyclohexylamino)-N-(quinolin-8-yl)propanamide (**II**) and N-(quinolin-8-yl)-2-(quinolin-8-yloxy) propanamide (**III**) by reacting with cyclohexylamine or 8-hydroxyquinoline respectively. The compound **I** was further converted to bromide and perchlorate salts **Ia** and **Ib** by reacting with hydrobromic acid or perchloric acid respectively.

The synthesis of N-(quinolin-8-yl)-2-(quinolin-8-yloxy)acetamide was already reported [23] while the N-(2-methoxyphenethyl)-2-(quinolin-8-yloxy)acetamide (**V**) was prepared by an analogous procedure by reacting 2-(2-methoxyphenyl)ethylamine with bromoacetlybromide followed by treatment with 8-hydroxyquinoline. The receptor bis(2-(quinolin-8-yloxy)ethyl)isophthalate (**VI**) was synthesized by reacting 8-hydroxyquinoline with bromomethylacetate followed by reduction of the ester by sodium borohydride to obtain an alcohol 2-(quinolin-8-yloxy) ethanol as an intermediate compound [24]. The 2-(quinolin-8-yloxy) ethanol on further treatment with isophthaloyl dichloride resulted in the formation of receptor **VI** (Scheme 2).

The reaction of *trans*-1,2-diaminocylohexane with bromoacetyl bromide followed by reaction with 8-hydroxyquinoline resulted in the formation of compound **VII** (Scheme 3). All the quinoline derivatives **I–VII** are characterised by recording their NMR, IR spectra and mass spectra. The crystal structures are determined wherever suitable crystals are found.

3.2. Fluorescence studies

The fluorescence emission of compound **I** is observed to be responsive towards amino acids. For example, it shows enhancement of emission intensity at 391 nm (λ_{ex} = 310 nm) for addition of L-alanine or DL-alanine (Fig. 1). We have not observed significant differences among the two isomers on binding to the ligand **I**.

The fluorescence spectra of the receptor **II** are also affected by mineral acids, amino acids, hydroxy acids, and simple carboxylic acids (Fig. 2). Here we have observed that the fluorescence intensity of **II** decreases on gradual addition of both mineral acids and amino acids. However, the change is very rapid in case of mineral acids than that of the amino acids. From these fluorescence titration curves we have calculated the binding constants of the various acids. The binding constant study clearly shows that receptor **II** binds mineral acids with much more affinity than that of the amino acids. The receptor **II** is also responsive to hydroxy acids such as ascorbic acid, mandelic acid, and tartaric acid.

Binding of receptor **II** was studied with two enantiomeric acids namely, D-mandelic acid and L-mandelic acid. However, we could not distinguish the two acids as in both the cases the fluorescence intensity of **II** decreases in the same order on gradual addition of the acids.

The fluorescence emission spectra of receptor **III** were studied in presence of different guests. The receptor **III** shows a remarkable decrease in fluorescence intensity at 510 nm on gradual addition of

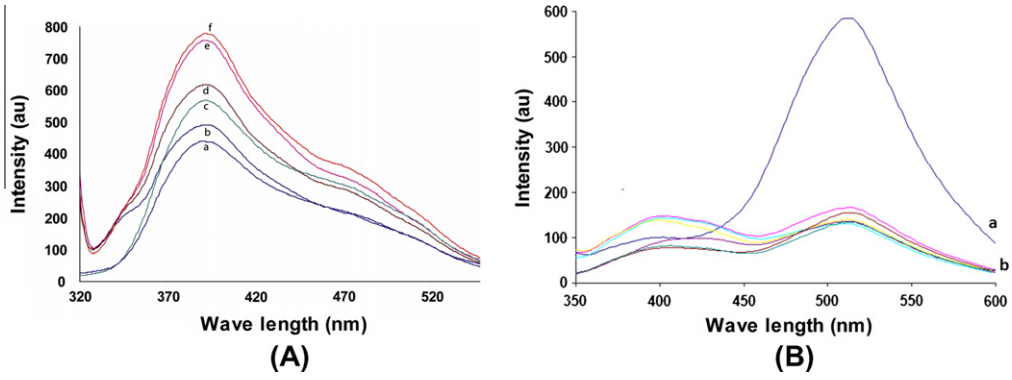

Fig. 6. (A) Fluorescence spectra (λ_{ex} = 310 nm) of: (a) **VI** (6.7×10^{-5} M in methanol); and after addition of amino acid (b) serin, (c) lysine, (d) methionine, (e) glycine and (f) alanine (100 μL of 10^{-2} M solution in methanol). (B) Fluorescence spectra of (a) **III** (2.5×10^{-5} M in methanol), (b) Fluorescence quenching of **III** after addition of amino acid (100 μL of 10^{-2} M solution in methanol) viz. glycine, metheonine, alanine, serin, and lysine.

amino acids (Fig. 3a). However, we have observed a mild enhancement of fluorescence emission intensity on addition of mineral acids to receptor **III** (Fig. 3b). The binding property of receptor **III** was studied with various hydroxy acids and carboxylic acids. It has been observed that receptor **III** is responsive towards both hydroxy acids, amino acids, mineral acids and simple carboxylic acids. With simple carboxylic acid like acetic acid it shows a gradual decrease in fluorescence (Fig. 3c). In case of fumaric acid along with the decrease in intensity at 510 nm a simultaneous increase in fluorescence intensity at around 420 nm is observed thereby forming an isoemissive point (the fluorescence curves are available in supplementary material).

On the other hand the fluorescence emission of receptor **V** is neither responsive to amino acids nor to hydroxy acids, but the fluorescence significantly changes on addition of dicarboxylic acids such as maleic acid and fumaric acid. The fluorescence intensity of **V** decreases on gradual addition of maleic acid and it passes through an isoemissive point at 457 nm as shown in Fig. 4.

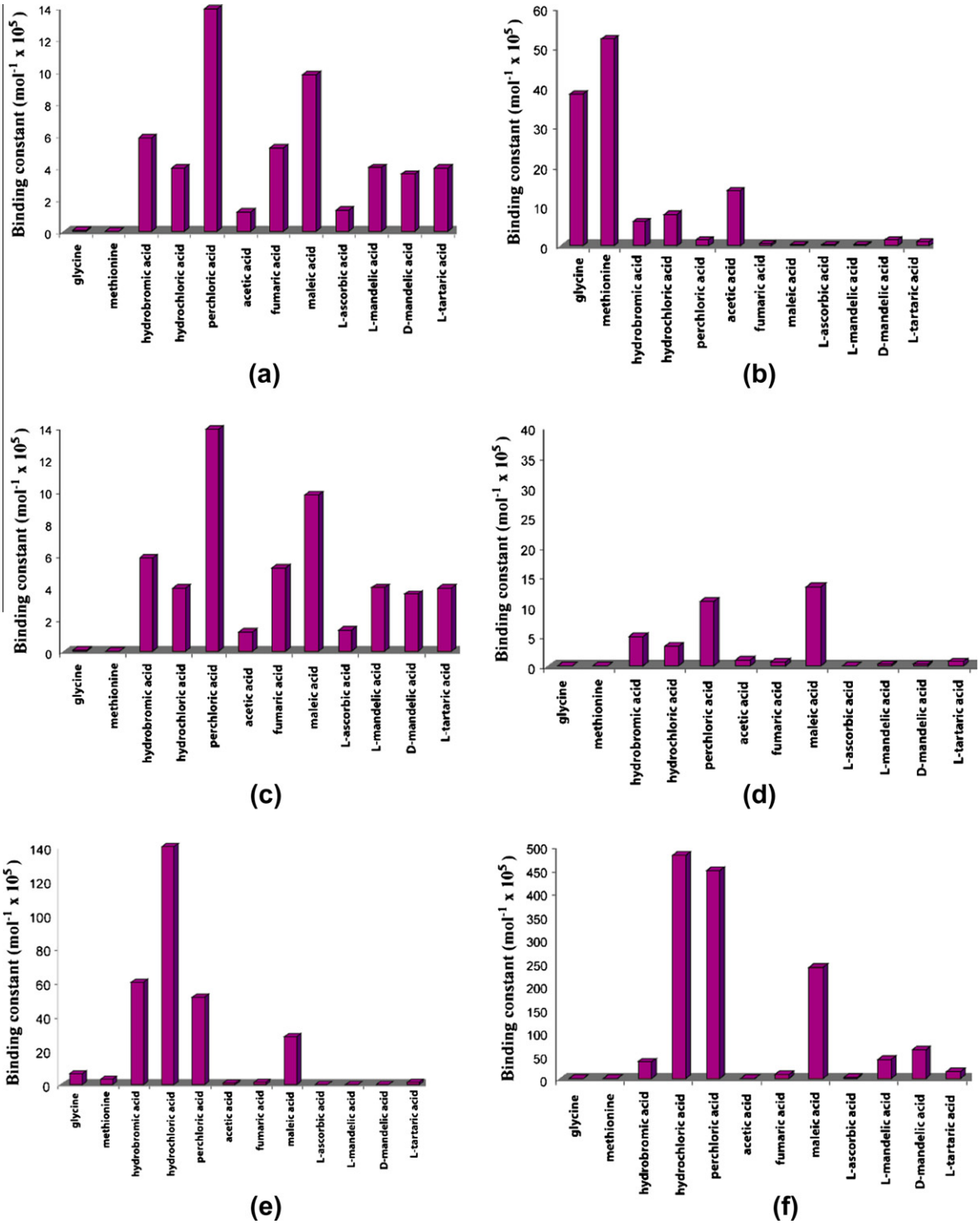

Fig. 7. Comparisons of binding constant of receptor: (a) **II**, (b) **III**, (c) **IV**, (d) **V**, (e) **VI**, (f) **VII** with different guest acids.

The fluorescence emission spectra of receptor **VI** is studied in presence of different carboxylic acids, amino acids, and mineral acids. A significant change in the fluorescence emission spectra of **VI** on treatment with mineral acid was observed. A methanol solution of **VI** shows fluorescence emission at 390 nm upon excitation at 310 nm. On gradual addition of HBr, HCl and $HClO_4$ a red-shift from 390 nm to 475 nm (85 nm shift) of fluorescence emission occurs. The spectral changes pass through an isoemissive point at 435 nm (Fig. 5a).

In order to differentiate the effect of amino acids over mineral acids on fluorescence emission, amino acid solutions viz. glycine or methionine were added gradually to a solution of receptor **VI** and the fluorescence spectra were recorded. We have observed an enhancement of the fluorescence emission intensity on addition of amino acids and unlike in the case of mineral acids no isoemissive point is observed (Fig. 5b). This difference in fluorescence spectra suggests different types of supramolecular aggregation of receptor **VI** with different guests. Comparing the study with mineral acids and with amino acids one can infer that the later case is not due to the simple protonation of **VI**.

Further we studied the binding properties of receptor **VI** with various acids including simple carboxylic acids (Fig. 5c) and a few hydroxy acids. At this point we have observed that receptor **VI** shows a very negligible affinity towards the hydroxy acids. However, receptor **VI** shows good affinity towards simple carboxylic acids. In case of simple carboxylic acids maleic acid behaves in a similar way to the mineral acids thereby passing through an isoemissive point whereas fumaric acid shows simple enhancement of fluorescence intensity as in the case of acetic acid. This may be because maleic acid prefers to form salt whereas fumaric acid prefers to form hydrogen bonded co-crystal [25]. The compound **IV** and **VII** are also fluorescence active and they show changes in fluorescence emission upon binding with acids. Since the results are analogous the figures are shown in supplementary materials and the binding constants are summarised in Table 2.

We have also studied the emission spectra in the presence of other amino acids such as serine, lysine and alanine. The relative intensity changes in the fluorescence emission spectra of the receptor **VI** is found to vary with different amino acids (Fig. 6A), whereas the changes in the intensity pattern of the receptor **III** is found to be similar with all the amino acids (Fig. 6B). In general the addition of amino acid leads to enhancement of fluorescence emission intensity of receptor **VI** and in case of such addition to receptor **III** fluorescence quenching is observed.

From the relative changes in the fluorescence emission due to guest host interactions, the binding constants for 1:1 host guest composition of all the systems are determined and these are listed in Table 2. The calculation of binding constant is done with the assumptions that 1:1 host–guest complex are formed and also being supported in majority of the cases by their crystal structures of the salts and co-crystals which are discussed in the next subsection.

Based on these results of binding constants a summary of comparative data on relative binding with respect to the hosts **II–VII** are shown in Fig. 7. It may be suggested that quinoline derivatives II–VII binds to various amino acids, mineral acids, carboxylic acids and hydroxy acids, but the binding abilities varies with structure of the parent receptor compound. Among all the receptors the receptor **VI** shows enhancement of fluorescence on interaction with amino acids and the other receptors show quenching. This receptor is highly sensitive towards both amino acid and mineral acid, thus it is less selective in binding. Furthermore this receptor is insensitive to hydroxy carboxylic acids other than tartaric acid. Tartaric acid being a dicarboxylic acid; the binding behaviour of this acid should be analogous to other dicarboxylic acids such as maleic acid which bind to this receptor. The mineral acid has also similar effect on all the receptors other than receptor **III** and in each case fluorescence quenching is observed. The receptor N-(quinolin-8-yl)-2-(quinolin-8-yloxy) propanamide **III** has high affinity to bind to amino acids in comparison to mineral acids. This makes the receptor **III** a promising candidate for recognising amino acid. Recently we have demonstrated that the nature of binding matters on the optical properties of receptors and based on this the mineral acid and organic acid can be distinguished by quinoline based receptors [23]. One of the important observations is the greater binding ability of amino acids in the case of **III** over **IV**. Both have similar structure other than an extra methyl group in **III**. So the steric effect of the methyl group is believed to make a transition state that is more favourable as illustrated in Fig. 8. Such state will be less favored in the case of **IV** as the quinoline part will have equal preferences for

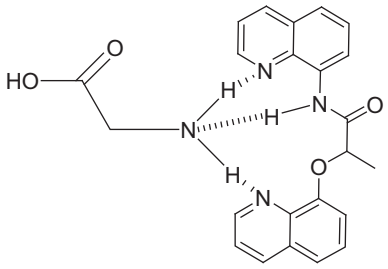

Fig. 8. H-bond interaction of receptor **III** with amino acid.

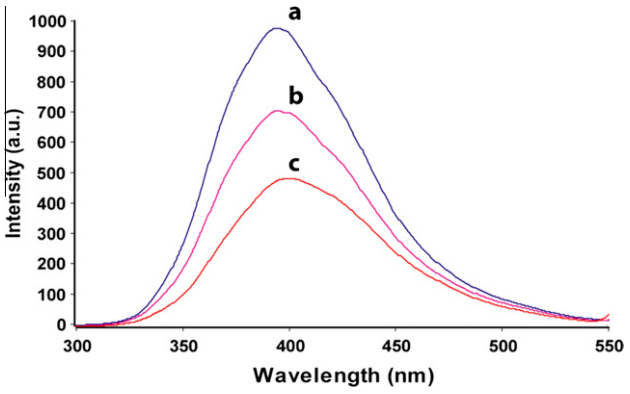

Fig. 9. (a) Emission spectra (λ_{ex} = 310 nm) of **II** (6.7×10^{-5} M in methanol); (b) emission spectra of **II** in mixed solvent of water and methanol (1:2); (c) emission spectra of **II** in mixed solvent of water and methanol (2:1).

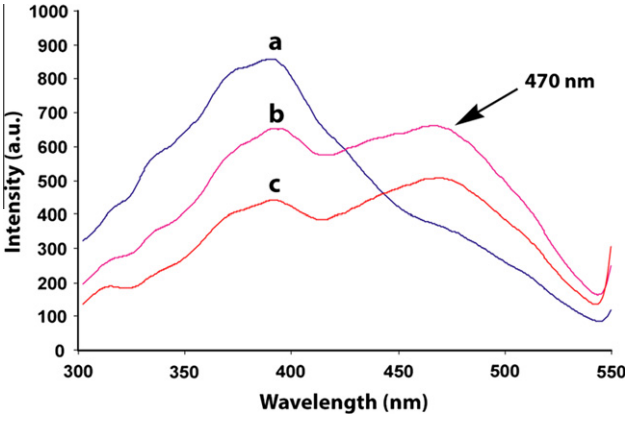

Fig. 10. (a) Emission spectra (λ_{ex} = 310 nm) of **VI** (6.7×10^{-5} M in methanol); (b) emission spectra of **VI** in mixed solvent of water and methanol (1:2); (c) emission spectra of **VI** in mixed solvent of water and methanol (2:1).

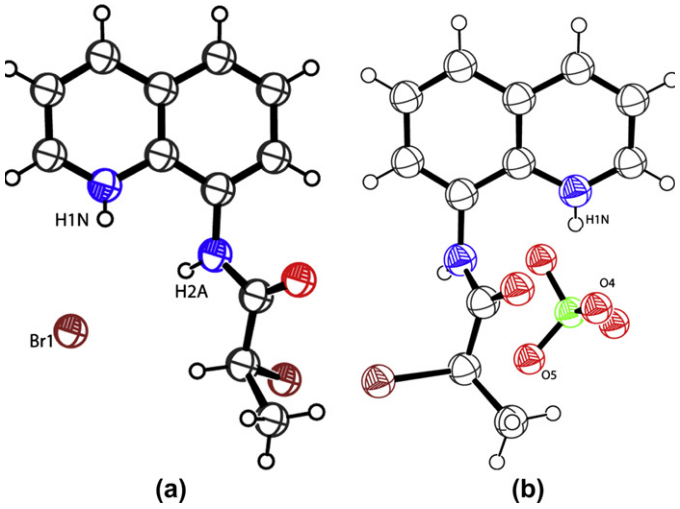

Fig. 11. Structure of: (a) bromide salt (**Ia**); (b) perchlorate salt (**Ib**) of protonated 2-bromo-N-(quinolin-8-yl) propanamide (Drawn with 50% thermal ellipsoid).

two oppositely directional orientations. This is also reflected in the crystal structure which is described in the next section. It is also to be noted that the receptor **VI** shows enhancement of fluorescence whereas in other cases quenching of fluorescence is observed. This is attributed to the interaction of lone pairs of the isophthalate ester groups in H-bonding to the amino acids making them unavailable for contributing to the fluorescence quenching of the quinoline unit. Such phenomenon is already observed earlier in crown ethers attached to fluorophores [29].

Since the molecules under consideration have quinoline unit, which has properties of drugs; study of the properties of these compounds in aqueous medium is necessary for finding out their applications. The compounds are generally insoluble in water so we studied the fluorescence emission spectra in different proportion of mixed solvents namely methanol and water. It is found that the compounds other than **VI**, have general tendencies to undergo fluorescence quenching on increasing proportion of water. As an illustrative case the change in fluorescence emission of methanolic solution of **II** with increase in water concentration is show in Fig. 9. This is attributed to hydrogen bonding with water molecules. In the case of **VI**, as water concentration increases there is a decrease in fluorescence emission of methanolic solution of it at 391 nm, with simultaneous generation of new emission peak at 470 nm (Fig. 10). This emission peak is similar to the additional emission peak observed on addition of mineral acid to **VI** (Fig. 5a) but the difference is that the amount of water needed for such process is in large excess in comparison to the amount of acid required for a similar growth of emission at 470 nm.

3.3. Structural study

The bromide and perchlorate salts of 2-bromo-N-(quinolin-8-yl) propanamide (**I**) are crystallized and its structures are shown in Fig. 11. These structures are of very much interest in understanding selective anion binding by amide containing receptors described earlier [26–28]. The solid state structure of these two cations have differences in orientation of the amide group, in the case of the bromide salt it lies in the plane of the quinoline ring whereas in the case of the perchlorate salt it is perpendicular to the quinoline plane. In both the cases the anions are coordinated with the protonated quinoline nitrogen through intermolecular hydrogen bonding. In case of the bromide salt (Fig. 11a) the anion is also coordinated with the amide hydrogen whereas in case of the perchlorate salt (Fig. 11b) the amide hydrogen is projected away from the coordinated anion.

Receptor **IV** crystallizes in the triclinic space group P-1 and has a bent structure as shown in Fig. 10b. The two quinoline rings lie almost perpendicular to each other, the dihedral angle between

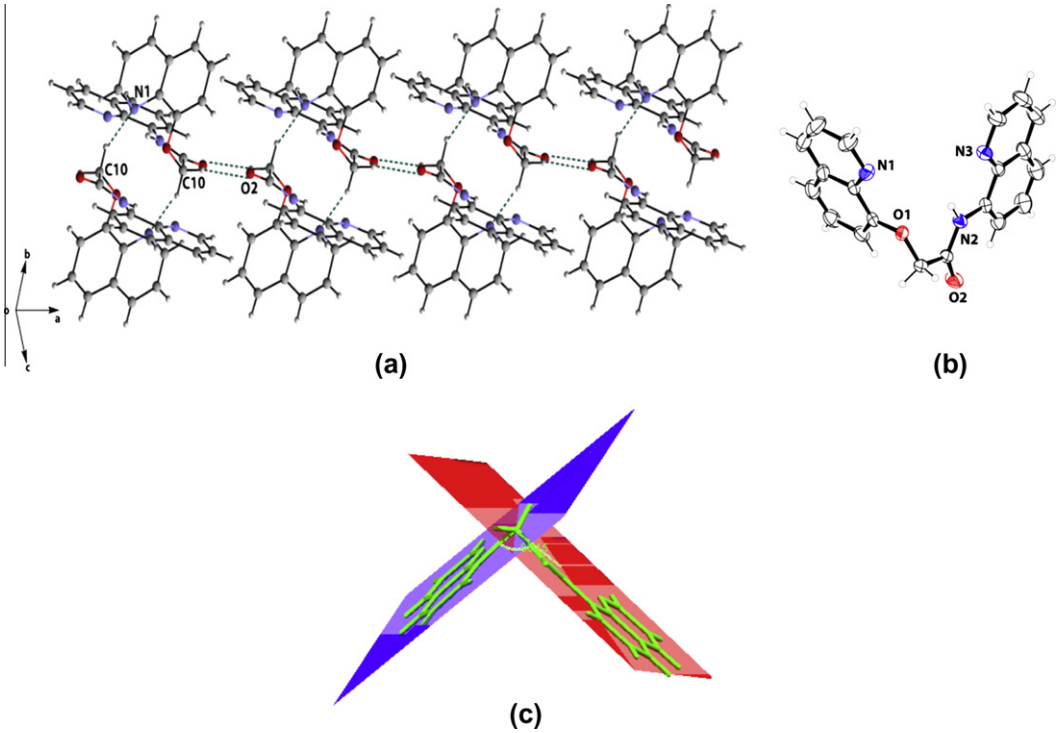

Fig. 12. (a) Short range interactions in **IV**, (b) ORTEP diagram of **IV** showing the asymmetric unit (drawn with 50% thermal ellipsoid), (c) dihedral angle between two planes containing the quinoline rings in **IV**.

Table 3
Hydrogen bond parameters of **IV**.

D–H···A	d_{D-H} (Å)	$d_{H\cdots A}$ (Å)	$d_{D\cdots A}$ (Å)	<D–H···A(0)
C(10)–H(10A)···O(2) [i]	0.97	2.51	3.4779(17)	174
C(10)–H(10B)···N1	0.97	2.63	3.327	138.6

i = $-x$, $1-y$, $-z$.

Table 4
Hydrogen bond parameters of **IVa**.

D–H···A	d_{D-H} (Å)	$d_{H\cdots A}$ (Å)	$d_{D\cdots A}$ (Å)	<D–H···A(0)
N(1)–H(1N)···O(9) [i]	0.887(16)	1.748(16)	2.620(3)	167.2(19)
N(2)–H(2A)···O(7)	0.86	2.60	3.373(2)	150
O(3)–H(3A)···O(5) [ii]	0.82	1.77	2.5854(18)	172
O(8)–H(8A)···O(6) [iii]	0.82	1.75	2.554(2)	166
O(9)–H(9A)···O(1) [iv]	0.841(17)	2.478(19)	2.983(2)	119(2)
O(9)–H(9A)···O(2) [v]	0.841(17)	1.867(18)	2.696(3)	168(2)
O(9)–H(9B)···O(6)	0.83(2)	1.90(2)	2.729(2)	172(3)
C(2)–H(2)···O(8) [vi]	0.93	2.52	3.445(3)	172
C(4)–H(4)···O(4) [vii]	0.93	2.48	3.223(3)	137

i = $1-x$, $-y$, $1-z$; ii = $-1+x$, y, z; iii = $-1+x$, y, z; iv = $1-x$, $-y$, $1-z$; v = $1-x$, $-y$, $1-z$; vi = x, $-1+y$, z; vii = $-x$, $-y$, $-z$.

the two planes containing the two quinoline ring is found to be 83.15° (Fig. 12c). The self assembly of the bent structure is stabilized by various weak interactions such as C–H···O interactions (C10–H10B···O2) and C–H···N interactions (C10–H10A···N1). The short range interactions in **IV** are shown in Fig. 12a. The hydrogen bond parameters are tabulated in Table 3.

Receptor **IV** was also crystallized with two carboxylic acids viz, fumaric acid (**IVa**) and maleic acid (**IVb**). The molecule **IVa** crystallizes in the triclinic space group P-1 with one half molecule of fumaric acid, one molecule of fumarate anion and one molecule of water in the asymmetric unit. It is observed that the orientation of the two quinoline rings changes on inclusion of the guest molecules thereby adopting an almost planar geometry. The dihedral angle between the planes containing the two quinoline rings changes to 4.9° as shown in Fig. 13a. Another interesting feature of the structure is that one fumaric acid molecule remains in the protonated form whereas the other molecule remains as an anion. The protonated and the unprotonated fumaric acid molecule forms a self assembly through intermolecular hydrogen bonding as shown in Fig. 13b. The fumaric acid molecule lies on an inversion centre with only half of the molecule contained in the crystallographic asymmetric unit, whereas in case of the deprotonated fumaric acid molecule, the entire molecule lies in the asymmetric unit (Fig. 13c).

The water molecule is held between one fumaric acid molecule and one molecule of receptor **IV** through intermolecular hydrogen bonding (N1–H1N···O9, O9–H9A···O2 and O9–H9B···O6). Fumaric acid molecule and the fumarate anion forms a self assembly through intermolecular hydrogen bonding (O8–H8A···O6 and O3–H3A···O5) as shown in Fig. 13d. The hydrogen bond parameters are tabulated in Table 4. From the Table 4 it can be inferred that the amide nitrogen (N2) forms a relatively weak intermolecular hydrogen bond with the oxygen atom (O7) of fumaric acid molecule in comparison with the other hydrogen bonds involved in the structure.

Unlike fumaric acid, maleic acid crystallises in a 1:1 ratio to form a salt with receptor **IV**. The salt of maleic acid (**IVb**) crystallises in the monoclinic space group P2(1)/n with one maleic acid anion and one water molecule in its asymmetric unit (Fig. 14b). In this case also it is found that the two quinoline rings lie almost in the same plane, the dihedral angle between the two plans containing the quinoline ring is found to be 1.9°. The receptor **IV** is held together by a number of π···π interactions (d_{C12-C1}, 3.358 Å; d_{C16-C4}, 3.361 Å; d_{C14-C6}, 3.473 Å). The maleic acid anion is further involved in a C–H···O interaction (C3–H3···O7) with the receptor **IV** and the water molecule is held by a strong hydrogen bond (N1–

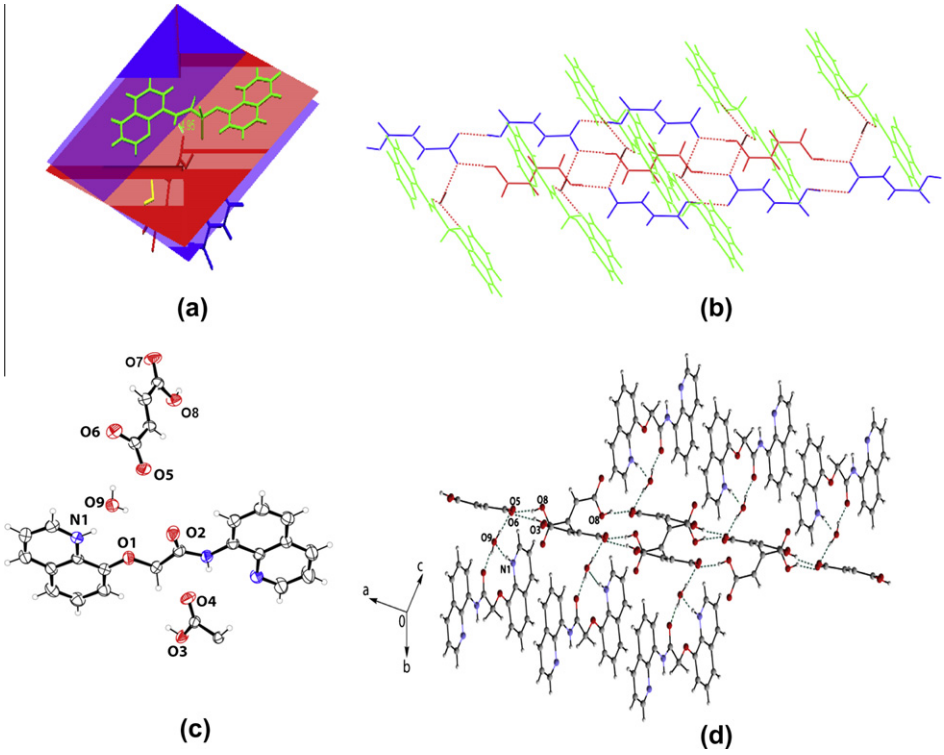

Fig. 13. (a) Dihedral angle between two planes containing the quinoline rings in **IVa**, (b) the two different types of symmetry non-equivalent fumaric acid molecules, (c) ORTEP diagram of the asymmetric unit of **IVa** showing the asymmetric unit (drawn with 50% thermal ellipsoid), (d) short range interactions present in **IVa**.

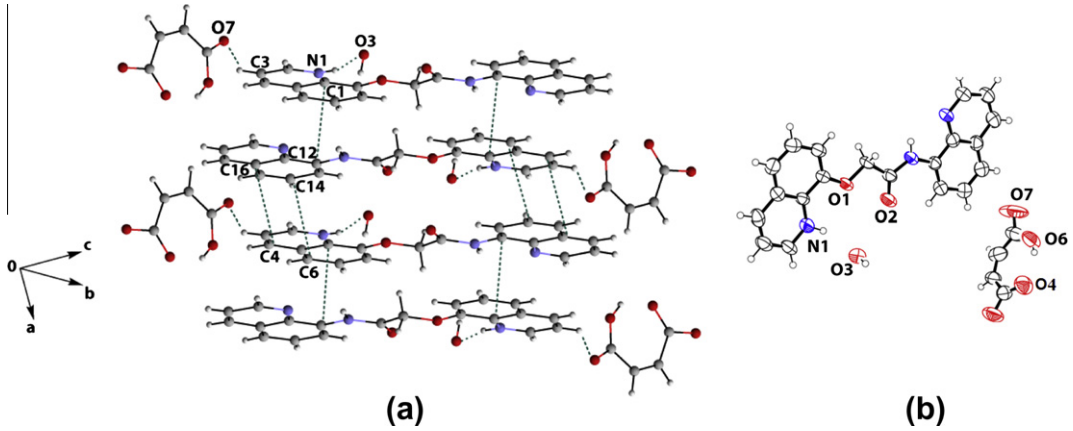

Fig. 14. (a) Short range interactions in **IVb**, (b) ORTEP diagram of **IVb** showing the asymmetric unit (drawn with 50% thermal ellipsoid).

Table 5
Hydrogen bond parameters of **IVb**.

D–H···A	d_{D-H} (Å)	$d_{H\cdots A}$ (Å)	$d_{D\cdots A}$ (Å)	<D–H···A(0)
N(1)–H(1N)···O(3) [i]	0.87(3)	1.81(2)	2.667(5)	170(5)
N(2)–H(2A)···O(5) [ii]	0.86	2.45	3.242(5)	153
O(3)–H(3A)···O(5)	0.82(2)	1.90(2)	2.724(7)	178(7)
C(3)–H(3)···O(7) [iii]	0.93	2.55	3.203(7)	128
C(10)–H(10A)···O(5) [iv]	0.97	2.43	3.030(5)	120
O(6)–H(6A)···O(4)	0.84(7)	1.77(7)	2.458(8)	138(6)

iI = 3/2 − *x*, −1/2 + *y*, 1/2 − *z*; ii = 1/2 + *x*, 1/2 − *y*, −1/2 + *z*; iii = 1/2 + *x*, −1/2 − *y*, −1/2 + *z*; iv = 1/2 + *x*, 1/2−*y*, −1/2 + *z*.

H1N···O3) with the protonated quinoline nitrogen (Fig. 14a). The hydrogen bond parameters are given in Table 5. In this case also it is observed that the amide nitrogen (N2) forms a relatively weak hydrogen bond with the oxygen atom (O5) of the guest acid than that of the other hydrogen bonds involved in the structure.

Table 6
Hydrogen bond parameters of **V**.

D–H···A	d_{D-H} (Å)	$d_{H\cdots A}$ (Å)	$d_{D\cdots A}$ (Å)	<D–H···A(0)
N(2)–H(2N)···O(5)	0.87(3)	2.09(3)	2.899(2)	155.0(19)
O(4)–H(4A)···O(2) [i]	0.91(3)	1.97(3)	2.874(2)	170(2)
O(4)–H(4B)···O(5)	0.82(4)	1.98(4)	2.794(2)	170(3)
O(5)–H(5A)···N(1)	0.86(3)	1.91(3)	2.763(2)	173(3)
O(5)–H(5B)···O(4) [ii]	0.88(4)	1.95(4)	2.813(2)	165(4)

i = −1 + *x*, *y*, *z*; ii = 1 − *x*, 1 − *y*, −*z*.

The crystal structures of two salts of **IV** with mineral acid namely, perchloric acid and tetrafluroboric acid are already reported [23]. By comparing with the structures of these salts it can be inferred that the geometry the receptor **IV** changes in the presence of guest.

The receptor **V** crystallises in the triclinic space group P-1 with two molecules of water in its asymmetric unit (Fig. 15b). Four

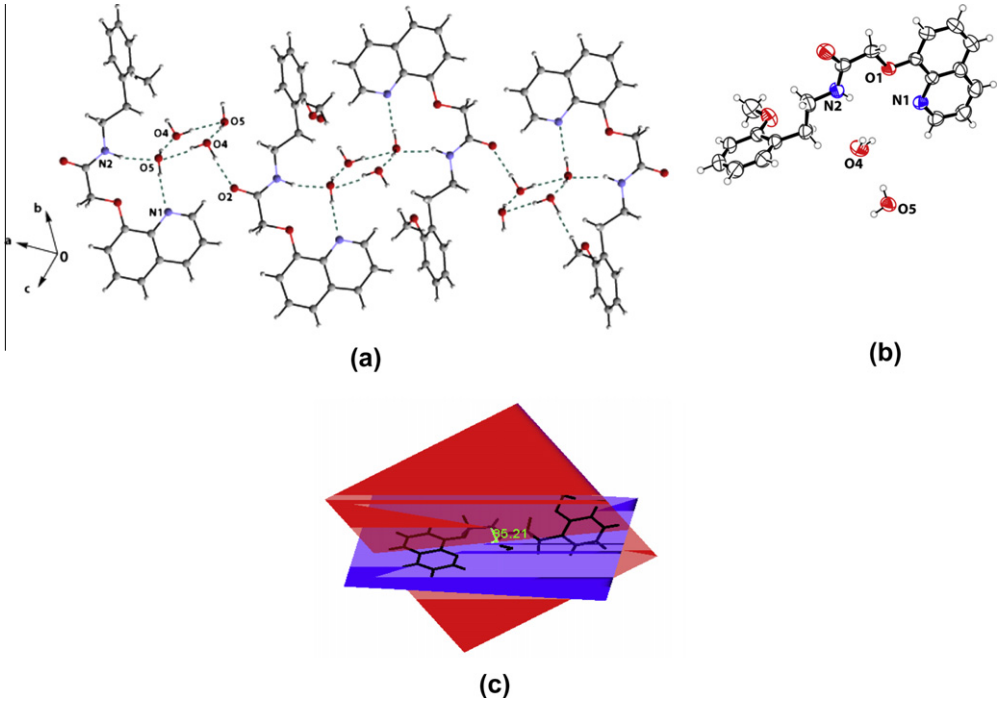

Fig. 15. (a) Short range interactions in **V**, (b) ORTEP diagram of **V** showing the asymmetric unit (drawn with 50% thermal ellipsoid), (c) dihedral angle between two planes containing the quinoline ring and the phenyl ring in **V**.

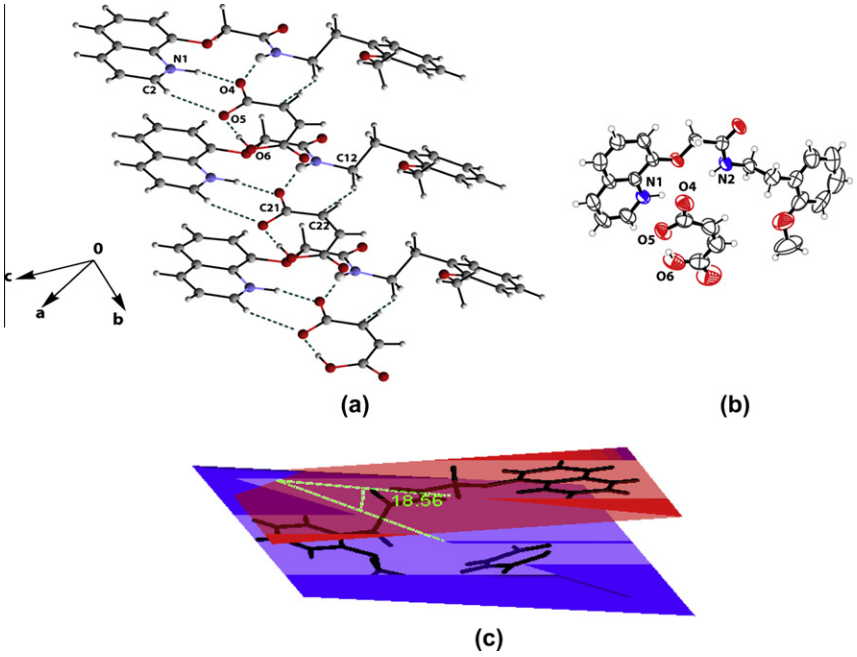

Fig. 16. (a) Short range interactions in **Va**, (b) ORTEP diagram of **Va** showing the asymmetric unit (drawn with 50% thermal ellipsoid), (c) dihedral angle between two planes containing the quinoline ring and the phenyl ring in **Va**.

Table 7
Hydrogen bond parameters of **Va**.

D–H···A	d_{D-H} (Å)	$d_{H\cdots A}$ (Å)	$d_{D\cdots A}$ (Å)	<D–H···A(0)
N(1)–H(1N)···O(4) [i]	1.03(3)	1.73(3)	2.729(4)	163(3)
N(2)–H(2N)···O(4) [ii]	0.85(3)	2.11(3)	2.915(4)	157(2)
O(6)–H(6A)···O(5)	0.84(3)	1.63(2)	2.461(4)	169(3)
C(2)–H(2)···O(5) [iii]	0.93	2.40	3.138(4)	136
C(8)–H(8)···O(2) [iv]	0.93	2.38	3.296(4)	170
C(10)–H(10B)···O(2) [v]	0.97	2.59	3.258(4)	126

i = *x*, 1 + *y*, *z*; ii = *x*, 1 + *y*, *z*; iii = *x*, 1 + *y*, *z*; iv = 1 − *x*, −*y*, −*z*; v = 1 − *x*, 1 − *y*, −*z*.

water molecules are held together in between two host molecules by hydrogen bonds (O4–H4A···O2, N2H2N···O5, and O5–H5A···N1) as shown in Fig. 15a. The hydrogen bond parameters are tabulated in Table 6. It is found that the quinoline ring and the phenyl ring lies in two different planes having dihedral angle 35.2° as shown in Fig. 15c.

The receptor **V** was then crystallised with two isomeric dicarboxylic acids namely, maleic acid and fumaric acid. In this case we have observed a 1:1 salt with maleic acid (**Va**) and a 1:2 co-crystal with fumaric acid (**Vb**).

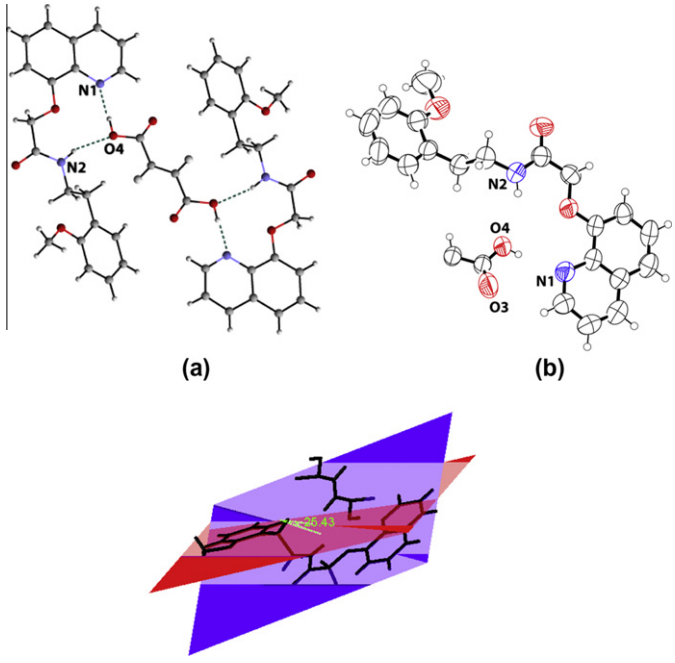

Fig. 17. (a) Hydrogen bonded structure of **Vb** showing encapsulation of one fumaric acid molecule by two molecules of receptor **V**, (b) ORTEP diagram of **Vb** showing the asymmetric unit (drawn with 50% thermal ellipsoid) (c) dihedral angle between two planes containing the quinoline ring and the phenyl ring in **Vb**.

Table 8
Hydrogen bond parameters of **Vb**.

D–H···A	d_{D-H} (Å)	$d_{H\cdots A}$ (Å)	$d_{D\cdots A}$ (Å)	<D–H···A(0)
N(2)–H(2A)···O(4) [i]	0.86	2.22	3.052(6)	163
O(4)–H(4A)···N(1) [ii]	0.82	1.84	2.651(5)	171

i = x, 3/2 − y, −1/2 + z; ii = x, 3/2 − y, 1/2 + z.

The salt **Va** crystallises in the monoclinic space group P2(1)/n. The protonated quinoline nitrogen atom forms a hydrogen bond with the oxygen atom of maleic acid anion (N1–H1N···O4). The maleic acid anion is further involved in various types of weak interactions (Fig. 16a) such as C–H···O interaction (C2–H2···O5), and hydrogen bonding interaction (N2–H2N···O4). The hydrogen bond parameters are tabulated in Table 7. In the structure of **Va** it is observed that the orientation of the two aromatic rings changes on inclusion of the guest molecule and the dihedral angle between the two planes containing the rings is found to be 18.5° (Fig. 16c). This change in orientation is favoured by the presence the ethylene spacer that involved in a C–H···π interaction with the maleic acid anion (C12–H12···C22).

The receptor **V** crystallises with fumaric acid leading to a 1:2 co-crystal (**Vb**) where one molecule of fumaric acid is held between two molecules of receptor **V** (Fig. 15a). The co-crystal **Vb** crystallises in monoclinic space group P2(1)/c, the fumaric acid molecule lies on an inversion centre with only half of the molecule contained in the crystallographic asymmetric unit (Fig. 17b). The fumaric acid molecule is held by intermolecular hydrogen bonding with receptor **V** (O4–H4A···N1 and N2–H2N···O4) as shown in Fig. 17a. The hydrogen bond parameters are tabulated in Table 8. From the Table 8 it is observed that the fumaric acid molecule forms a much stronger hydrogen bond with the quinoline nitrogen (N1) in comparison with the amide nitrogen (N2). In this case also it is found that the geometry of the two aromatic ring changes with the inclusion of the guest molecule, the dihedral angle between the two planes containing the rings is found to be 25.4° (Fig. 17c).

4. Conclusions

The non-planar geometry of the quinoline containing receptors, facilitates binding to anions; thereby enhances the interactions of such receptors with acids. The high affinity of N-(quinolin-8-yl)-2-(quinolin-8-yloxy)propanamide for amino acids is due to such effect. Poor affinity of N-(quinolin-8-yl)-2-(quinolin-8-yloxy)acetamide towards binding with amino acids, is related to the higher flexibility on the orientation of the quinoline ring. Based on the results of preferential binding of amino acid over hydroxy acids by receptor **VI** it may be stated that the overall preorganised structure of this receptor to have weak interactions with the corresponding anion of acid plays an important role in recognition of different acids. The structure of the self assemblies in the cases of fumaric acid and maleic acid with the amide functionalized quinoline receptors are guided by the geometry around the double bond of the acids; this is in accordance with earlier studies in related systems [23].

Supplementary material

The CIF of compounds are deposited to Cambridge Crystallographic Database and has the CCDC Nos. 790477-790482, 781136-781137.

Acknowledgements

The authors thank Department of Science and Technology New-Delhi, India for financial support. The author D.K. thanks Council of Scientific and Industrial Research, New Delhi, India for a Senior Research fellowship.

References

[1] J. Mao, H. Yuan, Y. Wang, B. Wan, M. Pieroni, Q. Huang, R.B. van Breemen, A.P. Kozikowski, S.G. Franzblau, J. Med. Chem. 52 (2009) 6966.
[2] P.R. Verhoest, D.S. Chapin, M. Corman, K. Fonseca, J.F. Harms, X. Hou, E.S. Marr, F.S. Menniti, F. Nelson, R. O'Connor, J. Pandit, C.P. LaFrance, A.W. Schmidt, C.J. Schmidt, J.A. Suiciak, S. Liras, J. Med. Chem. 52 (2009) 5188.
[3] G.X. Li, Z.Q. Liu, X.Y. Luo, Eur. J. Med. Chem. 45 (2010) 1821.
[4] H. Zeng, R. Cao, H. Zhang, Chem. Biol. Drug Des. 74 (2009) 596.
[5] E. Milner, W. McCalmont, J. Bhonsle, D. Caridha, D. Carroll, S. Gardner, L. Gerena, M. Gettayacamin, C. Lanteri, T. Luong, V. Melendez, J. Moon, N. Roncal, J. Sousa, A. Tungtaeng, P. Wipf, G. Dow, Bioorg. Med. Chem. Lett. 20 (2010) 1347.
[6] I. Deb, P. Paira, A. Hazra, S. Banerjee, P.K. Dutta, N.B. Mondal, S. Das, Bioorg. Med. Chem. 17 (2009) 5782.
[7] M. Albrecht, Triyanti, S. Schiffers, O. Osetska, G. Raabe, T. Wieland, L. Russo, Kari Rissanen, Eur. J. Org. Chem. (2007) 2850.
[8] S.F. Alshahateet, R. Bishop, D.C. Craig, F. Kooli, M.L. Scudder, CrystEngComm 10 (2008) 297.
[9] R.F. Semeniuc, T.J. Reamer, M.D. Smith, New J. Chem. 34 (2010) 439.
[10] A. Karmakar, R.J. Sarma, J.B. Baruah, CrystEngComm 9 (2007) 379.
[11] Y. Liu, K. Chen, D.S. Guo, Q. Li, H.B. Song, Cryst. Growth Des. 7 (2007) 2601.
[12] C.R. Bondy, P.A. Gale, S.J. Loeb, J. Am. Chem. Soc. 126 (2004) 5030.
[13] M.H. Filby, J.W. Steed, Coord. Chem. Rev. 250 (2006) 3200.
[14] A. Karmakar, J.B. Baruah, Supramol. Chem. 20 (2008) 667.
[15] A. Karmakar, R.J. Sarma, J.B. Baruah, CrystEngComm 9 (2007) 378.
[16] I. Tabushi, Y. Kuroda, T. Mizutani, J. Am. Chem. Soc. 108 (1986) 4514.
[17] A. Galan, D. Andreu, A.M. Echavarren, P. Prados, J. de Mendoza, J. Am. Chem. Soc. 114 (1992) 1512.
[18] Y. Kuroda, Y. Kato, T. Higashioji, J. Hasegawa, S. Kawanami, M. Takahashi, N. Shiraishi, K. Tanabe, H. Ogoshi, J. Am. Chem. Soc. 117 (1995) 10950.
[19] A. Metzger, K. Gloe, H. Stephan, F.P. Schmidtchen, J. Org. Chem. 61 (1996) 2051.
[20] G. Arena, A. Casnati, A. Contino, A. Magr, F. Sansone, D. Sciotto, R. Ungaro, Org. Biomol. Chem. 4 (2006) 243.
[21] I. Nicolas, S. Chevance, P.L. Maux, G. Simonneaux, Tetrahedron Asymmetry 21 (2010) 1788.
[22] J.W. Steed, J.L. Atwood (Eds.), Supramolecular Chemistry, John Wiley, New-York, 2000.
[23] D. Kalita, J.B. Baruah, CrystEngComm 12 (2010) 1562.
[24] J.C.S. da Costa, K.C. Pais, E.L. Fernandes, P.S.M. de Oliveira, J.S. Mendonça, M.V.N. de Souza, M.A. Peralta, T.R.A. Vasconcelos, ARKIVOC (2006) 128.
[25] D. Kalita, J.B. Baruah, J. Mol. Struct. 969 (2010) 75.
[26] S.A. de Silva, A. Zavaleta, D.E. Baron, O. Allam, E.V. Isidor, N. Kasbimura, J.M. Percarpio, Tetrahedron Lett. 38 (1997) 2237.
[27] S.Y. Liu, K.Y. Law, Y.B. Hea, W.H. Chan, Tetrahedron Lett. 47 (2006) 7857.
[28] A. Filippi, F. Gasparrini, M. Pierini, M. Speranza, C. Villani, J. Am. Chem. Soc. 127 (2005) 11912.
[29] S.O. Kang, R.A. Begum, K.B. James, Angew. Chem. Int. Ed. 45 (2006) 7882.